Solid-state ^{13}C NMR Study on Order → Disorder Phase Transition in Oleic Acid

Chikayo Akita,† Tatsuya Kawaguchi, Fumitoshi Kaneko*, and Hitoshi Yamamoto

Department of Macromolecular Science, Faculty of Science, Osaka University, Toyonaka, Osaka 560-0043, Japan

Masao Suzuki

Research Institute of Biological Materials, Heike 1459-16, Tohma, Nara 639-2154, Japan

Received: November 3, 2003; In Final Form: January 20, 2004

The reversible solid-state phase transition between the γ and α phases of oleic acid was followed by ^{13}C solid-state NMR spectroscopy. All peaks in the γ and α phases were assigned based on the corresponding crystal structures determined by X-ray diffraction method (Abrahamsson and Ryderstedt-Nahringbauer, 1962, and Kaneko et al., 1996). As to the transition behavior, there was a significant difference between the two hydrocarbon chains straddling *cis*-olefin group. On the $\gamma \rightarrow \alpha$ phase transition at 271 K, the methyl-sided methylene carbons exhibited upfield shifts due to the gauche effect. Characteristic peaks shifts due to the conformational change of the *cis*-olefin group were observed for *cis*-olefin carbons. On the other hand, the peaks due to carboxyl-sided chains showed no large shifts on this transition. Each oleic acid carbon atom showed a discontinuous decrease in T_1, except for the methyl carbon, which was in the extreme narrowing limit even in the γ phase. However, the T_1 values of the methyl-sided carbons were significantly smaller than those of the carboxyl-sided carbons in the α phase. The conformational disordering in the methyl-sided chains was accompanied by a remarkable increase of molecular motion in this moiety.

Introduction

The major part of natural lipids contain cis-unsaturated fatty acids as a building block. For example, most phospholipids in the biomembrane have a cis-unsaturated acyl chains at the second position of their glycerol backbone. It is well-known that the large steric hindrance of *cis*-olefin groups disturbs the close packing of hydrocarbon chains of phospholipids and keeps the mobility of biomembranes high, which activates the function of biomembranes at low temperatures.[1,2] Most lipid compounds having cis-unsaturated acyl chains have been found to exhibit a variety of aggregation states due to several conformations of *cis*-olefin group. It seems important to clarify the influence of cis-unsaturation on the aggregation states and physicochemical properties of lipid compounds.

The polymorphic studies provide concrete information about the relationship between structures and physical properties of lipid molecules. The polymorphism of a series of cis-monounsaturated fatty acids has been studied by means of X-ray diffraction and vibrational spectroscopy, and a variety of crystalline states and solid-state phase transitions have been found.[3−9] Through these polymorphic studies, it has been clarified that the conformation of the *cis*-olefin group is a key determinant of molecular shape, and therefore it governs the lateral packing modes of cis-unsaturated acyl chains in solid states.

So far most of the attention of the polymorphic studies on cis-unsaturated fatty acids has been focused on the aspects of molecular and crystal structures. The difference in dynamical properties between solid modifications has not been studied in detail. High-resolution solid-state NMR spectroscopy is nowadays widely used as a conventional method to investigate the dynamical properties and structures of various molecular aggregation systems. Although the dynamics of cis-unsaturated chains has been studied in solutions and melts,[10−12] there are few applications of high-resolution solid-state ^{13}C NMR spectroscopy to the polymorphism of lipid compounds containing cis-unsaturated chains.[13] We presume that the difficulty in analyzing solid-state NMR spectra of lipid compounds complicates such attempts. Except for the carbon atoms near end groups, most of the carbon atoms in hydrocarbon segments show overlapping peaks at almost the same chemical shifts. Compared with the peaks appearing in solution NMR spectra, the peaks of high-resolution solid-state NMR spectra are rather broad. Owing to various factors acting on each nucleus, the chemical shift of each carbon is rather different from that in solution NMR spectra. Furthermore, there are considerable spectral differences between polymorphs. Therefore, the detailed assignment of solid states in cis-unsaturated lipids is a tough task. However, if the factors determining the NMR spectra are elucidated, the information is widely applicable not only to the solid states of lipid compounds but also to biological systems containing cis-unsaturated hydrocarbon chains.

Oleic acid crystallized in two polymorphic phases,α (mp 13.3 °C) and β (mp 16.6 °C) depending on the crystallization condition. The α phase is obtained by rapid cooling and the β phase by extremely slow crystallization. Another polymorphic named the γ phase is also obtained by cooling the α phase below −4 °C.

One of the characteristics of cis-monounsaturated fatty acids is the existence of the reversible solid-state phase transition between the γ and α modifications; the γ phase transforms to the α phase on heating with a relatively large endothermic

* Corresponding author. Telephone: +81-6-6850-5453. Fax: +81-6-6850-5288. E-mail: toshi@chem.sci.osaka-u.ac.jp.
† E-mail: chikayo@chem.sci.osaka-u.ac.jp.

10.1021/jp037326p CCC: $27.50
Published on Web 03/12/2004

enthalpy change, e.g., about a fourth of the heat of fusion as that for oleic acid. So far the $\gamma \leftrightarrow \alpha$ phase transition has been found in many cis-monounsaturated fatty acids, such as oleic acid, palmitoleic acid, erucic acid, and so on.[6,7,14−17] We have studied the transition mechanism by means of IR and Raman spectroscopy and X-ray diffraction and have clarified that conformational disordering takes place selectively in the methyl-sided chain, accompanying a conformational change of the cis-double bond.[6,7] Although a stepwise increase in the mobility of the methyl-sided chain was also suggested, the dynamical properties of the γ and α phases are still not fully elucidated yet.

To clarify the mobility in individual parts of the cis-monounsaturated acyl chain, we followed the $\gamma \rightarrow \alpha$ phase transition of oleic acid with high-resolution solid-state ^{13}C NMR spectroscopy. By combining the information obtained by NMR spectroscopy such as chemical shifts and relaxation times with the previous results of crystal structural analyses and vibrational spectroscopic experiments, we accomplished the assignment of all peaks appearing in the γ and α phases and characterized the reversible solid-state transition from the aspects of dynamical property.

In this paper, we describe the experimental results in the following way. The first part is for the solution ^{1}H and ^{13}C NMR spectra of oleic acid, which we used as the reference for assigning the solid-state ^{13}C NMR spectra. The second part is devoted to a description of the spectral features and assignments for the γ and α phases. Finally, we discuss a few factors that have a significant influence on the spectra of cis-monounsaturated acyl chains.

Experiment Section

Samples. High purity samples (guaranteed more than 99.9%) of oleic acid were supplied by RIBM Japan.

Solution NMR Measurements. The NMR experiments were performed on Varian UNYTY INOVA 600 operating at 599.893 MHz (^{1}H) and 150.858 MHz (^{13}C) Larmor frequencies. Oleic acid was dissolved in deuterated chloroform. 1D ^{1}H spectra were recorded with spectral width of 9000.9 Hz and 64K data points, and 1D ^{13}C spectra with spectral width of 34632.0 Hz and 128K data points. 2D H−H COSY spectra were measured with 4K data points and spectral width of 9000.9 Hz in both F1 and F2 dimensions. HMQC and HMBC spectra were acquired with 512 × 4K and 1K × 4K data points and spectral widths of 9000.9 Hz (^{1}H) and 27472.5 Hz (^{13}C) in F1 and F2 dimensions, respectively.

^{13}C Solid-State NMR Measurements. ^{13}C CP/MAS spectra were measured by means of a Chemagnetecs CMX-300 spectrometer (JEOL) at 75.5 MHz with a CP/MAS accessory. The sample was contained in a 5 mm bullet-type rotor made of zirconium. The magic angle spinning (MAS) rate was set to 5 kHz to avoid the overlap of spinning sidebands. The T_1 value of methyl carbon was obtained with the inversion recovery sequence (T1xcpir pulse sequence) and the ones of the other carbons were obtained with the Torchia sequence (T1xcp pulse sequence). The numbers of scans and data points for the spectral width of 30 kHz were 16−32 and 8K, respectively. The $\pi/2$ pulse width was 3.5 μs. The cross-polarization (CP) contact time and the repeating time were 5 ms and 20−40 s, respectively. The temperature region was 284−193 K. 1D ^{13}C NMR spectra were obtained with spectral width of 30 kHz, with 16K data points, and the FID's were apodized by an exponential window function. A sine−bell window function was also used for determining the chemical shift of each peak.

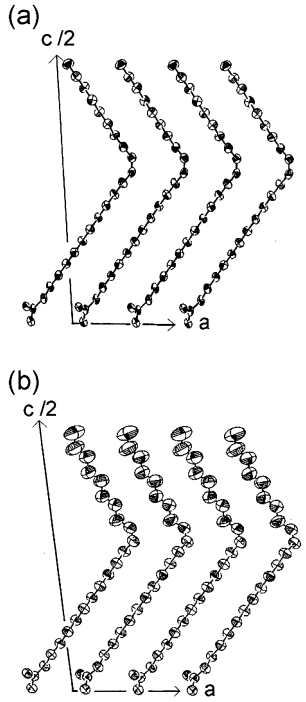

Figure 1. Crystal structure of the γ phase of erucic acid (a) and that of the α phase (b). Figure created from data taken from refs 8 and 6 with permission of the authors.

The Structure of the γ and α Phases. The structure of the γ phase of cis-monounsaturated fatty acids was determined in oleic acid and erucic acid using a single-crystal specimen.[3,8] There are four molecules in a unit cell belonging to a monoclinic system with space group $P2_1/a$. The dihedral angles of the C−C bonds next to the *cis*-C═C bond are recognized as *skew* and *skew′*, respectively. With this conformation, two hydrocarbon chains on both sides of *cis*-C═C bond are located perpendicular to the glide plane and form the O′∥ subcell (Figure 1a).

The structure of the α phase was determined in erucic acid using a single-crystal specimen[6] and also in oleic acid with a powdered specimen.[4] In the α phase, there are four molecules in a monoclinic unit cell of space group $P2_1/a$ as in the γ phase, but the portion between *cis*-C═C bond and methyl group shows a large difference from that of the γ phase; the C−C bond next to *cis*-C═C bond takes *trans* conformation and the hydrocarbon chain forms a subcell structure similar to the O⊥ subcell. On the other hand, the portion between *cis*-C═C bond and carboxyl group resembles that of the γ phase; the C−C bond next to *cis*-C═C bond takes *skew* (or *skew′*) conformation and the hydrocarbon chain forms the O′∥ subcell (Figure 1b).

With respect to thermal factors of carbon atoms, there is a large difference between the γ and α phases. In the γ phase, the thermal factors increase gradually toward the terminal methyl, but there is no conspicuous change between the methyl-sided and carboxyl-sided chains. On the other hand, the methyl-sided carbon atoms show significantly larger thermal factors than the carboxyl-sided ones in the α phase; they are becoming larger starting from *cis*-C═C bond toward the terminal methyl.

Results

1. Solution NMR. In the solid-state ^{13}C NMR spectra of long chain compounds, the peaks due to methylene carbons are relatively broad and overlap one another. As a result, it is quite difficult to interpret the spectrum in the region of 24−35 ppm. For reference purposes, we tried to assign all the peaks appearing in the solution ^{13}C NMR spectrum of oleic acid.

TABLE 1. Chemical Shifts of Oleic Acid in Solution ^{1}H and ^{13}C NMR Spectra and Solid-State ^{13}C Spectra of the γ and α Phases

	solution		solid							
	^{1}H	^{13}C	^{13}C in the γ phase at 213 K				^{13}C in the α phase at 279 K			
no.	shifts (ppm)	shifts (ppm)	shifts (ppm)	width (Hz)	ratio of intensities	T_1 (sec)	shifts (ppm)	width (Hz)	intensities	T_1 (sec)
1	–	180.5	181.6	37.1	–	358	181.2	12.1	–	173
2	2.34	34.12	35.2	22.7	1.56	271	35.0	17.5	0.84	178
3	1.63	24.66	26.2	26.7	1.13	311	26.0	18.3	1.00	164
4	1.29 ~ 1.32	29.14	32.8	24.4	1.00	425	32.6	19.9	1.00	129
5		29.07	34.4	29.4	1.29	651	34.3	16.2	1.04	85.4
6		29.05	34.2	27.6	1.20	635	34.2	17.5	0.94	60.0
7		29.68	34.7	37.4	5.24	368	33.7	16.2	0.93	40.7
8	2.01	27.16	30.5	23.1	2.16	357	30.7	17.5	1.04	33.1
9	5.34	129.7	129.6	34.9	–	355	129.6	15.4	–	35.8
10	5.34	130.0	129.6	34.9	–	355	130.6	16.2	–	40.6
11	2.01	27.22	30.5	23.1	2.16	357	28.6	8.7	0.96	13.4
12	1.29 ~ 1.32	29.78	34.7	37.4	5.24	368	33.3[a]	10.0	0.86	11.7
13		29.33					33.2[a]	10.0	1.12	13.6
14		29.53					33.1[a]	8.7	1.03	13.1
15		29.33					32.8	8.7	1.04	12.5
16		31.92	36.6	22.7	1.16	142	34.7	8.7	0.99	12.9
17	1.27	22.68	26.4	22.7	1.00	22.5	24.9	8.7	1.02	9.6
18	0.88	14.07	15.7	15.2	–	0.24	14.9	8.9	–	2.8

[a] At present these peaks are not assignable to a specific carbon atom in this part of the molecule.

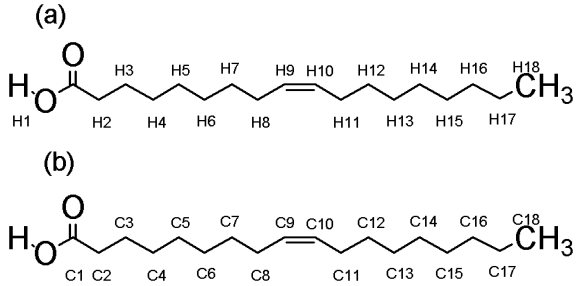

Figure 2. (a) Numbering of protons. (b) Numbering of carbons.

First, we assigned each peak of the ^{1}H NMR spectrum of oleic acid based on the results of the H−H COSY NMR experiment, as summarized in Table 1, where each proton is numbered as shown in Figure 2a. On the basis of this assignment and the experimental results of HMQC and HMBC, the assignments of all the peaks in the ^{13}C NMR spectrum were determined as summarized in Table 1 and Figure 2b. These assignments agree with those of methyl oleate and oleic acid in the previous studies.[18−21]

2. ^{13}C Solid-State NMR. Parts a and b of Figure 3 show the ^{13}C solid-state NMR spectra of the α and γ phases. The spectrum of the α phase is very complicated compared with that of the γ phase, as follows.

(1) In the γ phase, *cis*-C═C carbons exhibit only one peak at 129.6 ppm, while two peaks appear at 129.6 and 130.6 ppm in the α phase.

(2) The α phase exhibits more peaks in the range 24−36 ppm than the γ phase.

(3) With respect to the peaks due to methylene carbons in the α phase, the relative intensities change significantly with the delay time τ of the Torchia sequence, as shown in Figure 4a. For example, the peak at 28.6 ppm decays more quickly than that at 30.7 ppm. On the other hand, such differences in spin−lattice relaxation time are not observed in the γ phase (Figure 4b).

The contrast between α and γ can be interpreted based on their crystal structures. We consider that the lateral packing of hydrocarbon segments has a dominant influence on the peaks of hydrocarbon segments in the α and γ phases. It has been clarified that the chemical shifts of methylene carbons in hydrocarbon chains depend sensitively on the lateral packing; the peak due to polymethylene chains in the triclinic parallel (T∥), orthorhombic perpendicular (O⊥), and pseudohexagonal subcells appears at 34.0, 32.9, and 33.4 ppm, respectively. On the other hand, the amorphous region of polyethylene exhibits a peak at 32.0 ppm.[22−25]

In the γ phase, both the methyl-sided and carboxyl-sided chains form the O′∥ subcell structure, where the skeletal planes of hydrocarbon chains are parallel to each other as in the T∥ subcell. Therefore, the methylene groups in the central part of the both hydrocarbon chains are expected to show signals near 34 ppm. Indeed, an intense peak appears at 34.7 ppm.

On the transition to the α phase, only the O′∥ subcell of the methyl-sided chain changes to a relatively loose lateral packing similar to the O⊥ subcell. Therefore, the peaks due to the methyl-sided chain are expected to exhibit upfield shifts in the α phase. Actually a few intense peaks appear around 33.3 ppm. The difference in the lateral packing would affect the T_1 values of carbons. The loose lateral packing would activate the molecular motion of hydrocarbon chains, which results in the acceleration of spin−lattice relaxation. Accordingly, the methylene peaks having shorter T_1s in the α phase are assignable to the methyl-sided carbons. The peaks in the region of 32.8−33.3 ppm certainly relax faster than those in the region of 33.7−34.3 ppm. We referred to the thermal factors of each carbon atom determined through X-ray crystal structural analyses for the assignments of the methylene peaks.

The molecular conformation also affects chemical shifts of carbon atoms. The extent of a change in chemical shift is one of the important clues for the assignment. On the $\gamma \rightarrow \alpha$ transition, the conformational change at *cis*-olefin group and a conformational disordering around the terminal methyl take place, while no appreciable structural changes occur around the carbonyl group. Upfield shifts due to the gauche effect should be observed for the carbon atoms around the terminal methyl.

On the basis of the points discussed above and the results of solution NMR, the assignment of each peak was determined as shown in Figure 5, parts a and b, and Table 1 listed together with bandwidth, intensity ratio, and T_1. The intensity ratio of

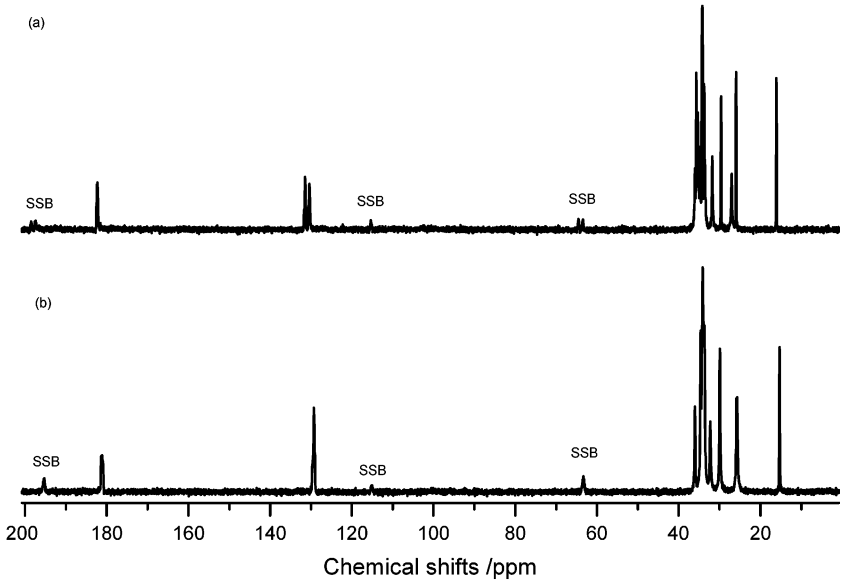

Figure 3. ^{13}C solid-state NMR spectrum of the α phase at 279 K (a) and that of the γ phase at 213 K (b).

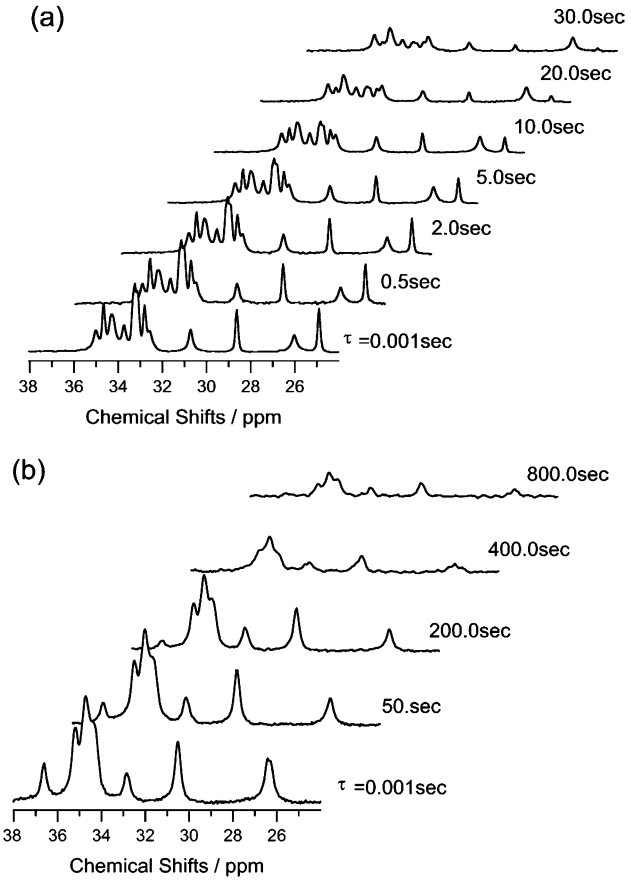

Figure 4. ^{13}C solid-state NMR spectrum of the α phase at 279 K as a function of delay time τ (a) and that of the γ phase at 213 K (b).

each peak is evaluated using the peak of C3 at 26.0 ppm in the α phase and the one of C4 at 32.8 ppm in the γ phase as an internal standard. We used the ratio as a measure of how many carbons contribute to a peak.

Spectral features of the α and γ phases are discussed below.

γ Phase. The peaks at 181.6 and 15.7 ppm are obviously ascribed to the carboxyl (C1) and methyl (C18) carbons. The peaks due to the carbons neighboring the carboxyl and methyl groups are clearly separated from those due to the midsection of polymethylene segments. The peak due to C2 appears at 35.2 ppm because of the magnetic deshielding of the carboxyl group, while the C3 and C4 carbons appear at 26.2 and 32.8 ppm because of the magnetic shielding of the carbonyl group. Concerning the carbons around the terminal methyl, the peaks due to C17 and C16 appear at 26.4 and 36.6 ppm. The peak at 26.3 ppm can be decomposed into two components at 26.4 and 26.2 ppm due to C17 and C3. We assign the peak at 26.4 ppm to C17, since it exhibits a significantly shorter T_1 than the peak at 26.2 ppm.

One of the spectral features of the γ phase is that several carbons of the methyl-sided chain appear at the same chemical shifts as those of the carboxyl-sided chain. With respect to the portion around *cis*-C═C bond, both the chains take the same conformation (*skew* or *skew′*) and subcell structure. The position relative to *cis*-C═C bond has a dominant influence on the chemical shifts of carbons in this portion. The C═C bond carbons C9 and C10 appear at 129.6 ppm, and the neighboring carbons C8 and C11 at 30.5 ppm. On the other hand, the central carbons of both the two chains are observed in the region around 34.5 ppm, which can be decomposed into three peaks at 34.7, 34.4, and 34.2 ppm with relative intensities corresponding to five, one, and one carbon atom, respectively. Besides having relatively long T_1s as shown in Table 1, the peaks at 34.4 and 34.2 ppm are also observed in the α phase, so that they are assigned to C5 and C6 of the carboxyl-sided chain. The peak at 34.7 ppm contains the C7, C12, C13, and C14 resonances.

α Phase. The peaks due to the methyl-sided carbons, C10−C18, show relatively large changes in chemical shifts, whereas the peaks due to the carboxyl-sided carbons, C1−C9, do not exhibit appreciable changes, as shown in Figure 5a and Table 1. The peaks associated with the portion around C═C bond are a typical example. Appearing as a singlet at 129.6 ppm in the γ phase, the *cis*-C═C carbons, C9 and C10, emerge as a doublet at 129.6 and 130.6 ppm. The C8 and C11 carbons next to *cis*-C═C bond are also observed separately at 30.7 and 28.6 ppm, respectively. The C16 and C17 carbons located near the methyl group show clear upfield shifts. The internal carbons of the methyl-sided chain shift to the region around 33.2 ppm, whereas those of the carboxyl-sided chain remain around 34.2 ppm.

All carbons except the methyl carbon C18 show shorter T_1 values in the α phase than in the γ phase. In the carboxyl-sided chain, T_1 gradually becomes shorter from the carboxyl group

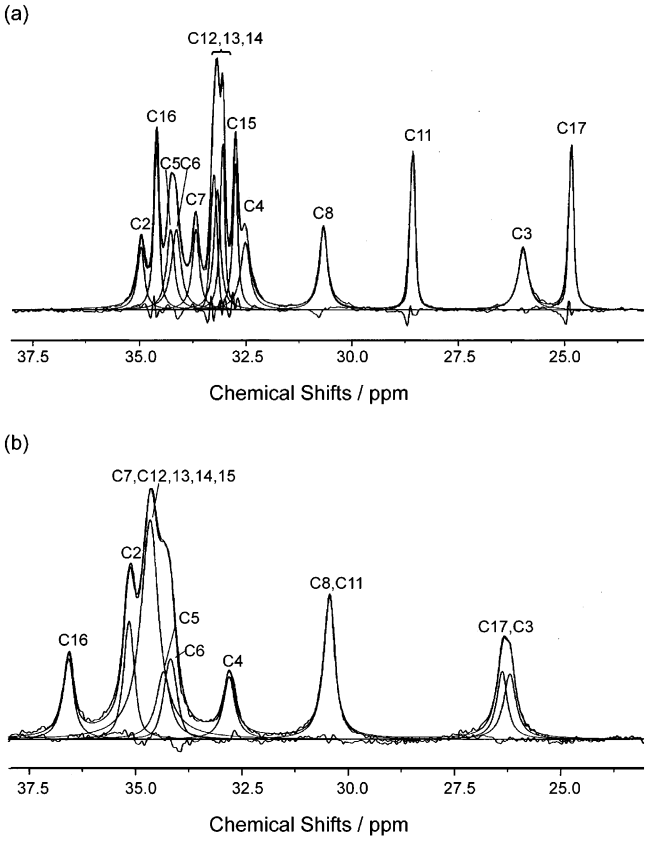

Figure 5. (a) Methylene region of ^{13}C NMR spectrum of the α phase at 279 K. (b) That of the γ phase at 213 K.

toward the olefin group, but it decreases abruptly at *cis*-C═C bond and remains almost constant in the methyl-sided chains. These tendencies of T_1s agree with the thermal factors obtained by X-ray crystal structural analysis.[6]

Discussion

Chemical Shifts of Carbons around Terminal Methyl. It is well-known that the chemical shift of carbon atom is influenced by the change in the electronic structure from the conformational change. In particular, the γ gauche effect[26,27] and vicinal gauche effect[28,29] are studied by both experiments and theoretical calcultions.[30−34] According to these studies, when the conformation of a C−C bond changes from trans to gauche, the peaks due to the carbons in proximity to the C−C bond show upfield shifts.

In this study, we have found that the carbons around the terminal methyl exhibit upfield shifts by about 1−2 ppm in the α phase compared with those of the γ phase (Figure 6). The chemical shifts of C15−C18 (methyl) carbons in the α phase resemble those of the γ-, β-, and α-methylene and methyl carbons in C_7H_{16} or C_8H_{18} in the urea inclusion compounds studied by Imashiro et al., respectively.[35,36] They concluded that the existence of the gauche conformation of the C_β-C_γ bond caused the upfield shifts for C_α (γ gauche effect), C_β and C_γ (vicinal gauche effect) compared with the corresponding carbons of *n*-alkanes taking all-trans conformation. A similar upfield shift of methyl group was also observed in the rotator phase of *n*-$C_{19}H_{40}$.[24]

Previous Raman spectroscopic studies on the α phase of cis-unsaturated fatty acids showed that the conformational disordering occurred at the C15−C16 and C16−C17 bonds upon $\gamma \leftrightarrow$ α phase transition.[5,6] Consequently, we can conclude that the upfield shifts of the C15, C16, and C17 carbons in the α phase are caused by the γ gauche effect and the vicinal gauche effect.

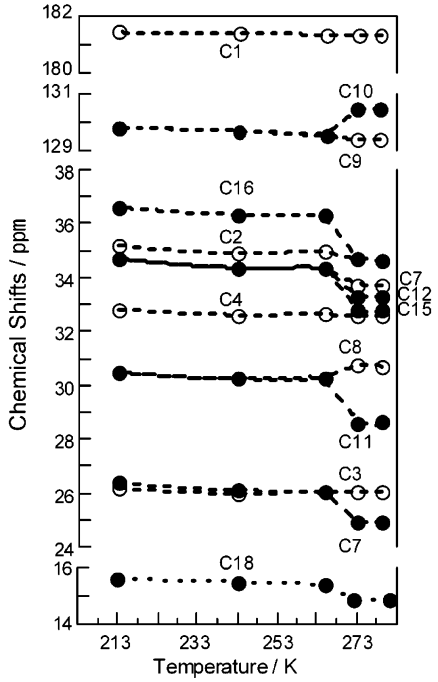

Figure 6. Temperature dependence of chemical shifts: (○) carboxyl-sided carbon; (●) methyl-sided carbon.

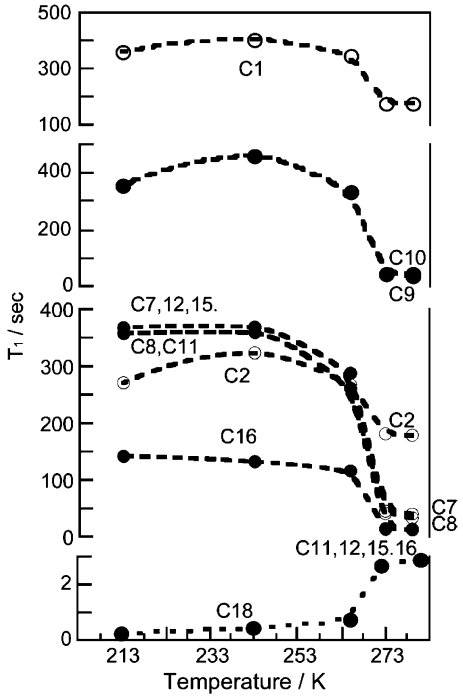

Figure 7. Temperature dependence of T_1s: (○) carboxyl-sided carbon; (●) methyl-sided carbon.

Transition Behaviors. Figure 6 shows the temperature dependence of the chemical shift of each carbon atom. Discontinuous changes are observed between 265 and 272 K sandwiching the $\gamma \leftrightarrow$ α transition point. The changes of the methyl-sided carbons are significantly larger than those of the carboxyl-sided carbons, which are consistent with the results of the previous X-ray and vibrational spectroscopic studies.

The same tendency is observed for the T_1s of carbons, as shown in Figure 7. T_1s become discontinuously short upon the $\gamma \rightarrow$ α transition, except that for the methyl carbon. In particular,

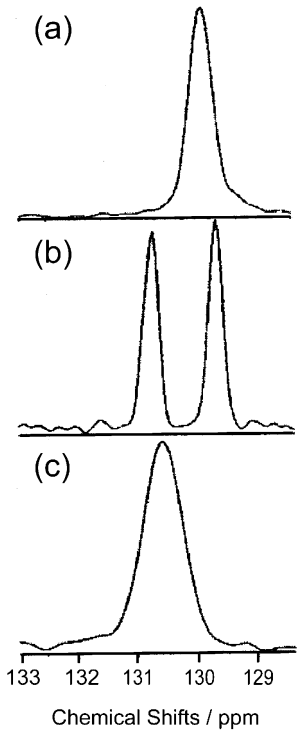

Figure 8. Olefin carbon region of the γ phase (a), the α phase (b), and the β phase (c).

the methyl-sided carbons exhibit a significant decrease in T_1. These changes imply that molecular motions become vigorous in the α phase especially in the methyl-sided chains accommodated in a relatively loose subcell. The T_1 of the methyl carbon C18, on the contrary, becomes longer at the transition point. It seems that the methyl carbon is in the extreme narrowing limit, which is consistent with the fact that the increase of T_1 is accompanied by a decrease in peak width which is approximately regarded as $1/T_2$. Therefore, the increase of T_1 means an increase in the mobility of the methyl group.

***cis*-Olefin Group.** The peaks due to *cis*-olefin and its neighboring carbons shift on the $\gamma \rightarrow \alpha$ phase transition, reflecting the conformational changes of the C−C bond next to *cis*-C═C bond in the methyl side. These peaks have a potential to be used as a probe for the conformational state of *cis*-olefin group in various lipid systems. In particular, the peaks of *cis*-olefin carbons, C9 and C10, are promising, since they are isolated from the signals of methylene carbons. As described in the previous section, these peaks would be a good indicator for the dihedral angle of the C−C bond attached to *cis*-C═C bond; the peak appears at 130.6 ppm for the *trans* conformation and at 129.6 ppm for the *skew* (or *skew*′) conformation. The spectrum of the β phase of oleic acid, where both the C−C bonds take *trans* conformation, is consistent with the above assignment; only one peak appears at 130.6 ppm as shown in Figure 8.

The neighboring carbons atoms, C8 and C11, also show characteristic changes on the $\gamma \rightarrow \alpha$ transition. The peak of C11 shifts from 30.5 to 28.6 ppm, while that of C8 shows a slight downfield shift by 0.2 ppm. With respect to the large upfield shift of C11, we infer that the intermolecular shielding effect of the *cis*-C═C bond, which has a large diamagnetism in the direction perpendicular to the plane containing the C−C═C−C group, is the main cause. In the γ phase, the *cis*-C═C bond is placed perpendicular to the basal plane of bimolecular layers, and the arrangements of the C8 and C11 atoms relative to the *cis*-C═C bond of the neighboring molecule related by a

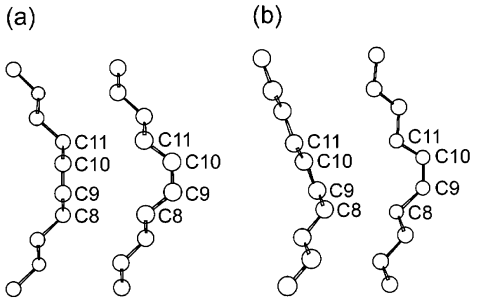

Figure 9. Arrangement of the C8 and C11 carbon atoms relative the *cis*-C═C bond of the neighboring molecule in the γ phase (a) and that in the α phase (b).

a glide plane are the same as shown in Figure 9a. However, the *cis*-C═C bond somewhat inclines toward the basal plane in the α phase, and the C11 and C8 atoms no longer keep the same arrangement relative to the proximal *cis*-C═C bond, as depicted in Figure 9b. Only the C11 atom intrudes in the shielding region of the *cis*-C═C bond. This configuration would cause only the C11 atom the upfield shifts, which consistent with the spectral changes on the $\gamma \rightarrow \alpha$ transition. Since the shielding and deshielding effect of *cis*-olefin group is complex,[37−42] the quantitative estimation of the intermolecular shielding effect on the chemical shift of C11 is difficult at present.

Acknowledgment. This works was supported by the 21 Century COE program.

References and Notes

(1) Stryer, L. *Biochemistry*; Freeman: New York, 1995; pp263−290.
(2) Voet, D.; Voet, J. G. *Biochemistry*; Wiley: New York, 1995; pp 277−329.
(3) Abrahamsson, S.; Ryderstedt-Naharingbauer, I. *Acta Crystallogr.* **1962**, *15*, 1261.
(4) Tandon, P.; Förster, G.; Neubert, R.; Wartewig, S. *J. Mol. Struct.* **2000**, *524*, 201.
(5) Kim, Y.; Strauss, H. L.; Snyder, R. G. *J. Phys. Chem.* **1988**, *92*, 5080.
(6) Kaneko, F.; Yamazaki, K.; Kobayashi, M.; Kitagawa, Y.; Matsuura, Y.; Sato, K.; Suzuki, M. *J. Phys. Chem.* **1996**, *100*, 9138.
(7) Kobayashi, M.; Kaneko, F.; Sato, K.; Suzuki, M. *J. Phys. Chem.* **1986**, *90*, 6371.
(8) Kaneko, F.; Yamazaki, K.; Kobayashi, M.; Kitagawa, Y.; Matsuura, Y.; Sato, K.; Suzuki, M. *Acta Crystallogr.* **1993**, *c49*, *100*, 1232.
(9) Kaneko, F.; Yamazaki, K.; Kitagawa, K.; Takahashi, K.; Kobayashi, M.; Kitagawa, Y.; Matsuura, Y.; Sato, K.; Suzuki, M. *J. Phys. Chem. B.* **1997**, *101*, 1803.
(10) Iwahashi, M.; Kasahara, Y.; Matsuzawa, H.; Yagi, K.; Nomura, K.; Terauchi, H.; Ozaki, Y.; Suzuki, M. *J. Phys. Chem. B.* **2000**, *104*, 6168.
(11) Seeling, J.; Seeling, A. *Q. Rev. Biophys.* **1980**, *13*, 19.
(12) Botchelor, J. G.; Prestegard, J. H.; Cushley, R. J.; Lipsky, S. R. *J. Am. Chem. Soc.* **1973**, *95*, 6358.
(13) Hindenes, J.-O.; Nerdal, W.; Guo, W.; Di, L.; Small, D. M.; Holmsen, H. *J. Biol. Chem.* **2000**, *275*, 6857.
(14) Suzuki, M.; Ogaki, T.; Sato, K. *J. Am. Oil. Chem. Soc.* **1985**, *62*, 1600.
(15) Suzuki, M.; Sato, K.; Yoshimoto, N.; Kobayashi, M. *J. Am. Oil. Chem. Soc.* **1988**, *65*, 1942.
(16) Sato, K. Yano, J.; Kawada, I.; Kawano, M.; Kaneko, F.; Suzuki, M. *J. Am. Oil. Chem. Soc.* **1997**, *74*,1153.
(17) Garti, N.; Sato, K. *Crystallization and Polymorphism of Fats and Fatty acids*; Marcel Dekker: New York, 1988; pp 227−263.
(18) Daniel, S.; John, P. W. *J. Am. Oil. Chem. Soc.* **1971**, *48*, 371.
(19) Batchelor, J. G.; Cushley, R. J.; Prestegard, J. H. *J. Org. Chem.* **1974**, *39*, 1698.
(20) Tulloch, A. P.; Mazurek, M. *Can. Lipids* **1976**, *11*, 228.
(21) Iwahashi, M.; Yamaguchi, Y.; Kato, T.; Horiuchi, T.; Sakurai, I.; Suzuki, M. *J. Phys. Chem.* **1991**, *95*, 445.
(22) Earl, W. L.; VanderHart, D. L. *Macromolecules* **1979**, *12*, 762.
(23) VanderHart, D. L. *J. Magn. Reson.* **1981**, *44*, 117.
(24) Ishikawa, S.; Kurosu, H.; Ando, I. *J. Mol. Struct.* **1991**, *248*, 361.
(25) Saito, H. *Magn. Reson. Chem.* **1986**, *24*, 835.

(26) Ellis, P. D.; Maciel, G. E.; McIver, J. W., Jr. *J. Am. Chem. Soc.* **1972**, *94*, 4069.
(27) Garber, A. R.; Ellis, P. D.; Seidman, K.; Schade, K. *J. Magn. Reson.* **1979**, *34*, 1.
(28) Anet, F. A. L.; Cheng, A. K.; Wagner, J. J. *J. Am. Chem. Soc.* **1972**, *94*, 9250.
(29) Anet, F. A. L.; Cheng, A. K. *J. Am. Chem. Soc.* **1975**, *97*, 2420.
(30) Ando, I.; Yamanobe, T.; Sorita, T.; Komoto, T.; Sato, H.; Deguchi, K.; Imanari, M. *Macromolecules* **1984**, *17*, 1995.
(31) Möller, M.; Gronski, W.; Cantow, H.-J.; Höcker, H. *J. Am. Chem. Soc.* **1984**, *106*, 5093.
(32) Drotloff, H.; Rotter, H.; Emeis. D.; Möller, M. *J. Am. Chem. Soc.* **1987**, *109*, 7797.
(33) Yamanobe, T.; Sorita, T.; Ando, I.; Sato, H. *Makromol. Chem.* **1985**, *186*, 2071.
(34) Ando, I.; Sorita, T.; Yamanobe, T.; Komoto, T.; Sato, H.; Deguchi, K.; Imanari, M. *Polymer* **1985**, *26*, 1864.
(35) Imashiro, F.; Maeda, T.; Nakai, T.; Saika, A.; Terao, T. *J. Phys. Chem.* **1986**, *22*, 5499.
(36) Imashiro, F.; Kuwahara, D.; Nakai, T.; Terao, T. *J. Chem. Phys.* **1989**, *90*, 3356.
(37) Jackman, L. M. *Application of Nuclear Magnetic resonance Spectroscopy in organic chemistry*, Pergamon Press: Oxford, England, 1959; p 112.
(38) Pople, J. A. *J. Chem. Phys.* **1962**, *37*, 53.
(39) Conroy, H, *Advances in Organic Chemistry: Method and Results*, Raphael, E. C., Taylor, E. C., Wynberg, H., Eds.; Wiley-Interscience, New York, 1960.
(40) Bothner-By, A. A.; Pople, J. A. *Annu. Rev., Phys. Chem.* **1965**, *16*, 43.
(41) ApSimon, J. W.; Craig, W. G.; Demarco, P. V.; Mathieson, D. W.; Saunders, L.; Whalley, W. B. *Tetrahedron* **1967**, *23*, 2357.
(42) Abraham, R. J.; Canton, M.; Griffiths, L. *Magn. Reson. Chem.* **2001**, *39*, 421.